



Modelling potential maize yield with climate and crop conditions around flowering

Simona Bassu^{a,*}, Davide Fumagalli^a, Andrea Toreti^a, Andrej Ceglar^a, Francesco Giunta^b, Rosella Motzo^b, Zuzanna Zajac^a, Stefan Niemeyer^a

^a European Commission, Joint Research Centre (JRC), Ispra, Italy

^b Dipartimento di Agraria, University of Sassari, Viale Italia 39, 07100, Sassari, Italy

ARTICLE INFO

Keywords:

Sowing date
Cultivar
Crop modelling
Maize grain yield
Climate change

ABSTRACT

Understanding, and then modelling, the effects of sowing date and cultivar on maize yield is essential to develop appropriate climate change adaptation strategies. Here we test the WOFOST model and a hybrid model, based on physiological crop conditions around flowering, against observed data collected during 4 years of field experiments in a Mediterranean environment under fully irrigated conditions. We simulate sowing date and cultivar responses by using 45-year historical meteorological records from the experimental weather station and future climate conditions till 2060 as projected by a set of regional climate models.

Both WOFOST and the hybrid approach reveal good performance in simulating average maize yield. However, the hybrid one outperforms WOFOST with respect to its responsiveness to changes in sowing date and cultivar.

These findings, besides stressing the importance of crop conditions around flowering in determining maize yield, point to lower yields (14%–17%, average reduction) under future climate conditions. The estimated losses may only be partially offset by changes in phenology and sowing dates.

1. Introduction

Optimizing the planting window is among the main low-cost adaptation strategies, with effects on both potential grain yield and its components (Cirilo and Andrade, 1994). Changing sowing date can adapt the growing season to optimally utilize available solar radiation, adjust crop phenological stages according to the period when temperatures are more suitable for growth, and avoid harmful stress events related to heat and water (Tsimba et al., 2013a).

Reductions in yield due to either late or early planting are well documented (Johnson and Mulvaney, 1980; Sorensen et al., 2000; Tsimba et al., 2013a, b; Caviglia et al., 2014; Bonelli et al., 2016; Zhou et al., 2017). In early sowing, the increase in growth duration may be offset by lower temperatures slowing canopy development and determining a lower value of mean accumulated incident photosynthetically active radiation intercepted by the crop (IPAR) up to silking (Otegui et al., 1996). Conversely, a delay in sowing date can reduce the number of kernels per square meter due to the less favorable photo-thermal conditions during the critical period for grain set and grain filling (Tsimba et al., 2013a; Bonelli et al., 2016). The optimal combination of

sowing date and cultivar depends on local environmental and climate conditions (Olson and Sander, 1988; Shaw, 1988; Bonelli et al., 2016).

Process-based crop models have been widely used, together with field experiments, to optimize sowing date not only under current climate conditions (Otegui et al., 1995, 1996; Hammer and Broad, 2003; Anapalli Saseendran et al., 2005; Yang et al., 2006; Andrade et al., 2010; Grassini et al., 2011) but also as an adaptation strategy for future climate conditions (Olesen and Bindi, 2002; Torriani et al., 2007; Tojo Soler et al., 2007; Giannakopoulos et al., 2009; Vučetić, 2011; Liu et al., 2013; Zhao et al., 2015; Ma et al., 2017; Srivastava et al., 2018; Ciscar et al., 2018).

Despite the widespread use of crop models' to analyze crop responses to changes in sowing date and cultivar, only a few works have explored their effects on yield variability (Hammer and Broad, 2003; Messina et al., 2009). These studies showed, for example, how the stability of the harvest index approach for yield prediction is affected by both the sowing date and the cultivar choice. Bonelli et al. (2016), in their field experiments, observed that by delaying the sowing date the variation in biomass was not balanced by the variation in grain yield, highlighting the inconsistency of a constant-value harvest index approach.

* Corresponding author.

E-mail address: simona.bassu@ec.europa.eu (S. Bassu).

<https://doi.org/10.1016/j.fcr.2021.108226>

Received 4 December 2020; Received in revised form 29 June 2021; Accepted 5 July 2021

Available online 16 July 2021

0378-4290/© 2021 The Authors. Published by Elsevier B.V. This is an open access article under the CC BY license (<http://creativecommons.org/licenses/by/4.0/>).

Partitioning methods based on constant values (and the resulting yield estimates) may be affected by similar issues.

The partitioning approach is the one currently used by the WOFOST crop model (De Koning and Van Diepen, 1992; Supit et al., 2010; Wolf, 1993; Wolf and Van Diepen, 1995; Supit et al., 2012). Total dry matter growth is partitioned according to fixed distribution factors, defined as a function of development stage. After flowering, the daily net photosynthesis together with the duration of grain filling mainly determine yield. Within this approach, sowing date and cultivar may affect the amount of dry matter allocated to grain yield mainly through their effects on grain filling duration. Without distinguishing among yield components, this approach (despite being robust for simulating yield response to different environments) may lack sufficient details to describe genotypic and sowing date effects. Indeed, it does not consider the grain demand, i.e. the potential capacity of the kernels to use the available assimilates in the post-anthesis period (Echarte and Andrade, 2003; Hammer and Broad, 2003).

Maize grain yield is highly correlated with kernel set (Otegui et al., 1995), which is very sensitive to environmental conditions during silking (Cirilo and Andrade, 1994). Thus, an alternative approach to the partitioning method can be built on crop physiological conditions during flowering (e.g. light interception; Otegui et al., 1995). In this way, the variability in crop production across different sowing dates and cultivars mainly depends on the variability in the amount of photosynthetically active radiation intercepted by the crop around flowering time.

Resource availability per kernel around flowering also determines kernels' size and the capacity to use assimilate in the post-anthesis phase, with an effect on the potential seed dry weight and the achievable yield. Therefore, yield can be described using both potential kernels number and size, where the latter one can be calculated by using crop conditions around the period of kernel number determination (Gambín et al., 2006).

On the other hand, variations in assimilates supply during grain filling may affect kernel weight (Andrade and Ferreiro, 1996). The physiological conditions of maize plants during the grain filling period may become as relevant as the ones around flowering, particularly when sowing is delayed (Bonelli et al., 2016). Variations in climatic conditions during grain filling, associated to varying sowing dates, have been also reported among the main factors influencing final yield in the temperate zone of China (Zhou et al., 2017). Moreover, cultivars with a longer growing cycle length might be able to reduce negative effects of climate change (Liu et al., 2013).

The aim of this study is to explore whether, in Mediterranean climates, yield variability across sowing dates and cultivars can be entirely explained by the source limitation around flowering.

Two modelling approaches are here used: one fully based on the WOFOST model, relying on the partitioning approach; another one based on a hybrid approach, developed combining WOFOST with a model built on physiological crop conditions around flowering. These two modelling approaches are here tested against observed data collected during 4-year field experiments in a Mediterranean environment under fully irrigated conditions.

2. Materials and methods

2.1. Field experiments

Different combinations of sowing date and cultivar were tested in 2015, 2016, 2018, 2019 (no experiments were run in 2017) at the experimental maize field of Santa Lucia (39.9 °N - 8.5 °E; 15 m elevation; Sardinia, Italy) under optimum management, i.e. in absence of nutrients' limitations and under potential water conditions. This experimental site is characterized by Mediterranean climate with a long-term average seasonal rainfall of about 500 mm, mainly accumulating between October and April. Mean monthly temperatures range from 10 °C in January and February to 24.5 °C in August. The soil is clay-loam with

plant available water holding capacity of 250 mm on a volume basis to the maximum rooting depth of 130 cm. The territory is characterized by intensive dairy and grain farming with maize growing in irrigated conditions mainly from April until September. Treatments during the experiments were randomized in a split-plot design with three replications. Sowing date treatments were assigned to the main plots and cultivars to the subplots. Plots consisted of: ten rows 0.70 m apart, 4.5 m long in 2015 and 2016; sixteen rows 0.70 m apart, 10 m long in 2018 and 2019. Cultivars were hybrids of various FAO maturity groups (Jugenheimer, 1958), having increasing anthesis and maturity requirements. Each FAO group is identified with a number; the lower the number, the fewer heat units that are required to reach grain maturity. Details on the management of the experiments are shown in Table 1. Trials were sown on: 29 April, 20 May and 23 June in 2015; 27 April, 19 May, and 23 June in 2016; 9 July in 2018; 6 May and 6 June in 2019. Plots were fertilized with 200 kg N ha⁻¹ and irrigated by drip irrigation. Scheduling was based on maize evapotranspiration (ETc) calculated from the actual ETo measured in a nearby Class A evaporation pan and the FAO crop coefficients for maize (Allen et al., 1998). The cumulative water applied (irrigation plus rainfall) was close to maize ETc throughout the growing season in all the experimental years.

2.2. Measurements

Crop phenological staging was assessed regularly on ten tagged plants. Flowering was registered when first tassels were visible on these plants. Crop above-ground biomass was measured at anthesis date, kernel dough stage and physiological maturity by hand cutting ten consecutive plants from the central row of each sub-plot. Dry weight was determined on these samples after oven drying for 48 h at 65 °C. Measurements of leaf area index (LAI), fraction of photosynthetically active intercepted radiation and the correspondent radiation extinction coefficient (K) were made non-destructively using a plant canopy analyzer (LAI-2000, LI-COR, Lincoln, NE) twice a week across all the growing cycle.

Grain yield and number of plants per unit area were determined after physiological maturity by hand, harvesting all ears and counting the plants from an area of 14 m² per plot. Kernel number and kernel weight were determined in years 2016, 2018, and 2019 on the ten-tagged plants by a manual trash of the ears. Grain yields refer to oven-dry (65 °C) and reported as 0 % grain moisture content.

2.3. Meteorological data

Meteorological records (daily values of incoming solar radiation, daily maximum and minimum temperatures, daily total rainfall, and mean wind speed) were retrieved from a meteorological station located in the field. 45 years of data (1974–2019) are available. Vapor pressure was estimated according to Allen et al. (1998).

Table 1

Field experiments conducted at Santa Lucia, Sardinia, Italy in 2015, 2016, 2018, and 2019.

Year	Cultivar	FAO class	Sowing density (Plants m ⁻²)	Sowing dates
2015	PR36B08	300	10	29 April, 20 May, 23 June
2015	PR33M15	500	10	29 April, 20 May, 23 June
2015	P1501	600	9	29 April, 20 May, 23 June
2015	PR31Y43	700	8	29 April, 20 May, 23 June
2016	PR35F38	400	10	27 April, 19 May, 23 June
2016	PR33M15	500	10	27 April, 19 May, 23 June
2016	P1501	600	9	27 April, 19 May, 23 June
2016	PR31Y43	700	8	27 April, 19 May, 23 June
2016	P2948W	800	8	27 April, 19 May, 23 June
2018	PR31Y43	700	8	9 July
2019	PR39F58	200	8	6 June
2019	PR31Y43	700	8	6 May and 6 June

2.4. Crop model

The first modelling approach here used is fully based on WOFOST (Van Diepen et al., 1989). This model computes daily biomass accumulation and distribution in crop organs using a photosynthesis approach. WOFOST derives the daily growth rate by the availability of assimilates, that is obtained by simulating canopy photosynthesis. Both growth and maintenance respiration processes are explicitly accounted for in determining dry matter production. WOFOST assumes grain yield being source-limited and dependent on dry matter accumulation before and after anthesis. The model estimates grain yield by applying a set of partitioning factors (depending on the development stage); they correspond to the fraction of assimilates assigned to the various organs.

Crop yield is here simulated under potential conditions and is expressed in dry weight. Therefore, no water-stresses (e.g. drought, water-logging) and biotic factors are assumed to affect crop yield that is only determined by temperature, day length, solar radiation, and cultivar.

2.5. Model calibration

The WOFOST maize parameterization was taken from the EC-JRC Monitoring Agricultural ResourceS (MARS) Crop Yield Forecasting System (MCYFS; Micale and Genovese, 2004; Lazar and Genovese, 2004; Genovese and Bettio, 2004). To calibrate the model at the Sardinian experimental site, phenology, LAI and biomass time course, and yield were calibrated sequentially (Boote et al., 1999; Ceglar et al., 2011). All the 4-year experimental data were used for the calibration. An automatic python procedure, minimizing the Mean Absolute Error (MAE) via Truncated Newton Constrained (TNC) algorithm, was run for the calibration.

The cultivar-dependent calibration of the phenological parameters TSUM1 and TSUM2 (accounting for the thermal time to anthesis and maturity, respectively) was performed as well. The obtained TSUM1 values vary between 595 °C d and 804 °C d, while TSUM2 values range from 749 °C d to 925 °C d across all the cultivars (Supplementary Material, Table S1). It is worth to note that flowering is assumed to be photoperiod independent (IDSL = 0).

The extinction coefficient for diffuse visible light (KDIFF, decreased to 0.5 with respect to the default MCYFS value) was chosen according to the experimental values measured in 2016. The specific leaf area (being function of the development stage) and the lower threshold temperature for ageing leaves were, respectively, decreased and increased (with respect to the MCYFS settings) to minimize the MAE between the observed and the simulated LAI across the growing season of all the treatments. The initial total crop dry weight was increased (with respect to the MCYFS value) to get more accurate simulations of dry matter on the base of the MAE between observed and simulated biomass across the growing seasons. Finally, the developmental stage from which above-ground dry matter is completely allocated to storage organs was modified (DVS = 1.34 for FOTB = 1.0) to minimize the MAE of the harvest index. The calibrated parameters are reported in Table 2. These values lie inside the plausible ranges reported in previous studies (Boogaard et al., 1998; Boons-Prins et al., 1993; Ceglar et al., 2011), with the exception of the lower threshold temperature for ageing leaves (a higher

value was estimated). The crop model input parameters are all listed in the Supplementary material Table S1.

2.6. The hybrid approach: Otegui-Gambín

The second modelling approach here evaluated is a hybrid one combining the WOFOST-simulated above-ground biomass, LAI, and anthesis date with the yield estimation method proposed by Otegui and Bonhomme (1998) and Gambín et al. (2006). Hereafter, the hybrid approach is simply named Otegui-Gambín (Fig. 1). The yield estimation, based on the climatic conditions around flowering, is obtained by multiplying the kernel number per m² by the kernel weight. The kernel number per plant (KN plant⁻¹) is estimated by using the intercepted photosynthetically active radiation (IPAR) near anthesis (Otegui and Bonhomme, 1998):

$$KN \text{ plant}^{-1} = 97 + 15 * IPAR \text{ plant}^{-1} \quad (1)$$

To calculate the IPAR in eq. (1), the incoming solar radiation is first converted into photosynthetically active radiation (PAR) using a 0.45 multiplication factor (Monteith, 1965). Then, the IPAR is derived as follows:

$$PAR * fIPAR \quad (2)$$

Where

$$fIPAR = 1 - \exp(-K * LAI) \quad (3)$$

The value of the extinction coefficient K is given by the average of the K values derived from the fraction of intercepted radiation and the LAI measured in 2016. The LAI values are the ones simulated by WOFOST between -227 °C d and 100 °C d (Otegui and Bonhomme, 1998) from the predicted anthesis at the experimental site. Thermal time values are calculated by using a base temperature of 8 °C (Ritchie and NeSmith, 1991). Since the Otegui and Bonhomme (1998) original approach is on a per-plant basis, we used the population density of the 4-year experiment.

The potential kernel weight is determined by using the approach of Gambín et al. (2006) with the local calibration of the required functions done according to the plant growth rate (as simulated by WOFOST around flowering) and the observed kernel weight. Simulated biomass accumulation from pre-silking (-15 days) to post-silking (+15 days) is divided by the thermal time interval. Plant growth rate (PGR) around flowering (mg °C d⁻¹) is then derived from the plant growth rate (PGR) per kernel (mg °C d⁻¹ kernel⁻¹) around flowering as follows:

$$PGR_{\text{per kernel around flowering}} = 0.7 * 10^{-3} * PGR_{\text{around flowering}} + 0.3773 \quad (4)$$

where $PGR_{\text{per kernel around flowering}}$ is calculated as the ratio between $PGR_{\text{around flowering}}$ and the observed kernel number. The kernel weight (mg kernel⁻¹) is derived as:

$$\text{Kernel weight} = 522.24 * PGR_{\text{per kernel around flowering}} - 8.7108 \quad (5)$$

The effective kernel weight after the grain filling period is the result of the potential kernel growth rate, calculated from the potential grain size (Gambín et al., 2006), and the effective grain filling duration. The latter one begins with the linear phase of the grain filling period, i.e. 200

Table 2
WOFOST crop parameters calibrated and used for all the maize cultivars.

Name	Description	Unit	Value	Range	Literature
KDIFF	Extinction coefficient for diffuse visible light	-	0.5	0.44-0.65	Ceglar et al. (2011)
SLATB00	Specific leaf area at development stage 0	ha Kg ⁻¹	0.00236	0.0022-0.0035	Ceglar et al. (2011)
SLATB078	Specific leaf area at development stage 0.78	ha Kg ⁻¹	0.0008	0.00070-0.0042	Boogaard et al. (1998)
TBASE	Lower threshold temperature for ageing leaves	°C	12.65	-10-10	Boogaard et al. (1998)
TDWI	Initial total crop dry weight	kg ha ⁻¹	137	0.50-300	Boogaard et al. (1998)
DVS for FOTB = 1.0	Developmental stage from which above-ground dry matter is completely allocated to storage organs	-	1.34	1.20-1.30	Ceglar et al. (2011)

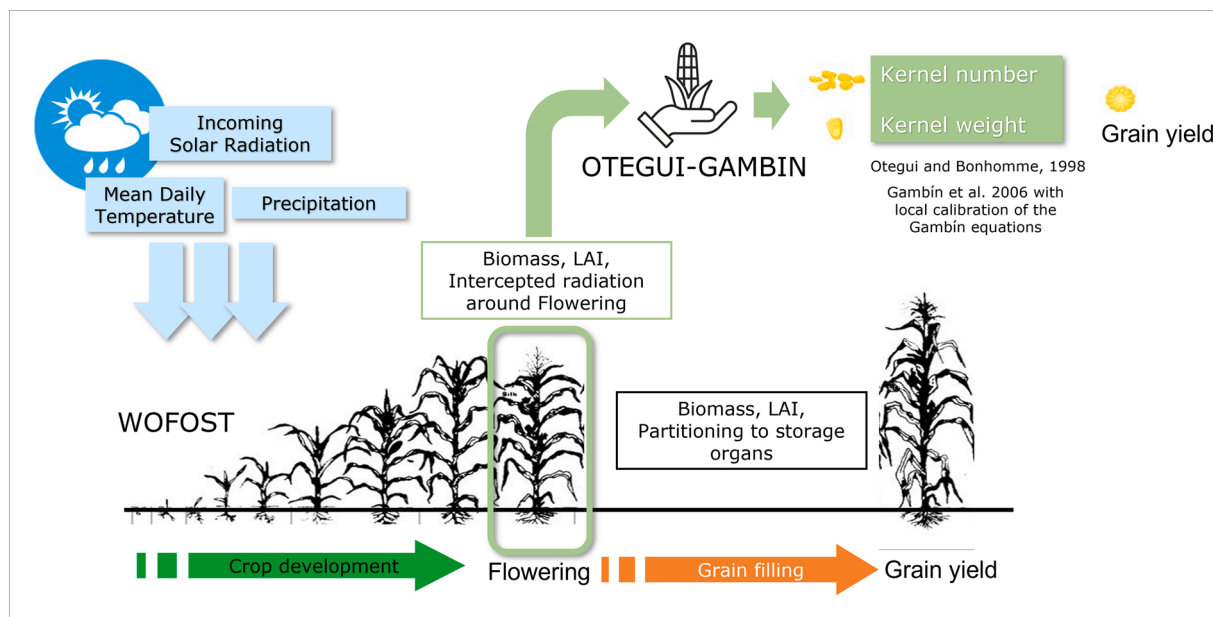


Fig. 1. Schematic representation of the Otegui-Gambín hybrid approach.

°C d after the anthesis, assuming the kernel weight before the linear phase being negligible and set to 3.9 % of the maximum kernel weight (Echarte et al., 2006). Daily assimilation cannot exceed the potential kernel growth per day. The assimilation rate is also corrected for sub-optimal average daytime temperatures. Finally, translocation contributes to yield formation no more than 15 % of leaf biomass and 20 % of stem biomass at the start of grain filling.

2.7. Model evaluation

The accuracy of the two modelling approaches, WOFOST and Otegui-Gambín, is evaluated against the 4-year field experiment by using the root mean squared difference (RMSD) between observed and simulated data. Furthermore, modelling efficiency (EF; Willmott, 1982) for the 1 to 1 ($y = x$) line is determined by measuring the true deviation of the estimates from observations (Mitchell, 1997). The modelling efficiency is defined as:

$$EF = 1 - \frac{\sum_{i=1}^n (O_i - S_i)^2}{\sum_{i=1}^n (O_i - \bar{O})^2} \quad (6)$$

Where \bar{O} is the mean of the observed values, O_i and S_i are the observed and simulated values, respectively. A positive EF value indicates that the model outperforms the simplest predicting system based on the mean of the observations. The maximum EF (i.e., 1) is reached when the simulated values are perfectly equal to the measured data. Negative EF values indicate that the model perform worse than the simplest predicting system.

The bias is evaluated by calculating the mean difference between measured and simulated data with the Mean Bias Error (MBE) that immediately provides information on overestimation (positive values) or underestimation (negative ones). Finally, the coefficient of determination (r^2) of the linear regression between simulated and observed values provides information on the ability of the model in capturing the range of variation and the variability of the measured values.

2.8. Long-term simulation experiment

To study the effect of sowing date and cultivar on crop production

both WOFOST and Otegui-Gambín were run for cultivars 400, 500, 600, 700, 800 with the 45-year historical meteorological records from the Santa Lucia weather station. Six fixed sowing dates (15th and 30th of each month from April to June) were analyzed.

2.9. Climate change projections 2021–2060

To consider the impact of climate change on maize production, climate projections from 5 regional climate model/global climate model combinations (RCMs/GCMs) from the EURO-CORDEX Initiative (Jacob et al., 2014), bias-adjusted by Dosio (2016), were retrieved. These RCMs are: CCLM4-8-17 driven by CNRM-CERFACS-CNRM-CM5; CCLM4-8-17 driven by ICHEC-EC-EARTH; WRF331 F driven by IPSL-IPSL-CM5A-MR; RCA4 driven by MOHC-HadGEM2-ES; RCA4 driven by MPI-M-MPI-ESM-LR. Bias-adjustment was performed on daily temperatures (maximum, minimum, and mean) and total precipitation (Dosio, 2016). Concerning the other parameters, needed to run the WOFOST model, targeted approaches were applied (Hristov et al., 2020). Global radiation from each RCM/GCM was evaluated against a set of high quality observational data sets, and in case of poor performance replaced with the one derived from the bias-adjusted parameters and the simulated cloud cover (Hristov et al., 2020 and references therein). Relative humidity was derived from the bias-adjusted daily parameters, while daily mean speed was used with no further post-processing (due to known difficulties in having high quality observational data sets covering large regions). The high-end emission scenario RCP8.5 was selected. It corresponds to a rising radiative forcing pathway leading to 8.5 W/m² (≈ 1370 ppm CO₂ equiv.) by 2100 (Riahi et al., 2011). Besides the baseline period (i.e. 1986–2005), two future time periods were selected: 2021–2040 and 2041–2060.

3. Results

3.1. Field experiments

The weather conditions in all the analyzed years were overall similar and representative of the mean climate conditions of Santa Lucia (Fig. 2). Two exceptions are, however, well visible in Fig. 2: the noticeable lower global radiation from May to August 2018 and the lower maximum temperatures from August to October 2015. It is also worth to highlight the highest minimum temperature in July 2015.

Concerning the measured maize yield, their values range between 20.6 t ha⁻¹ (2016) and 8.3 t ha⁻¹ (2019). Sowing dates induced significant variations in the observed yields, with the exception of 2016 (Supplementary material, Table S2). Observed yields decreased by delaying the sowing with the exception of the increased yield observed delaying the sowing from April to May in 2015. Yields of the tested cultivars differed significantly in 2015 ($P < 0.05$), 2016, and 2019 ($P < 0.001$). Cultivar 500 was the most productive one, whereas cultivar 200 was the least productive.

The range of variation in the number of kernels per unit area was 3613–5517, depending on the sowing date and the cultivar maturity group, with the highest values observed for the earliest sowing dates and the latest cultivar. Kernel weight ranged between 219 and 344 mg kernel⁻¹ with cultivar 700 showing the highest values.

Overall, the treatments with the highest yield and kernel number per m² showed the highest IPAR around anthesis, recorded (during the highest yielding year 2016) with cultivar 800 and the first sowing date among the ones tested. The largest yield variation across the sowing dates was observed in the year having the largest variation in IPAR around flowering, i.e. 2015. The highest IPAR and yield levels of 2016 (associated with lower yield variability) suggest that a sort of saturation threshold for these cultivars was reached during this experimental year. Indeed, further increases in IPAR could only produce weaker yield response.

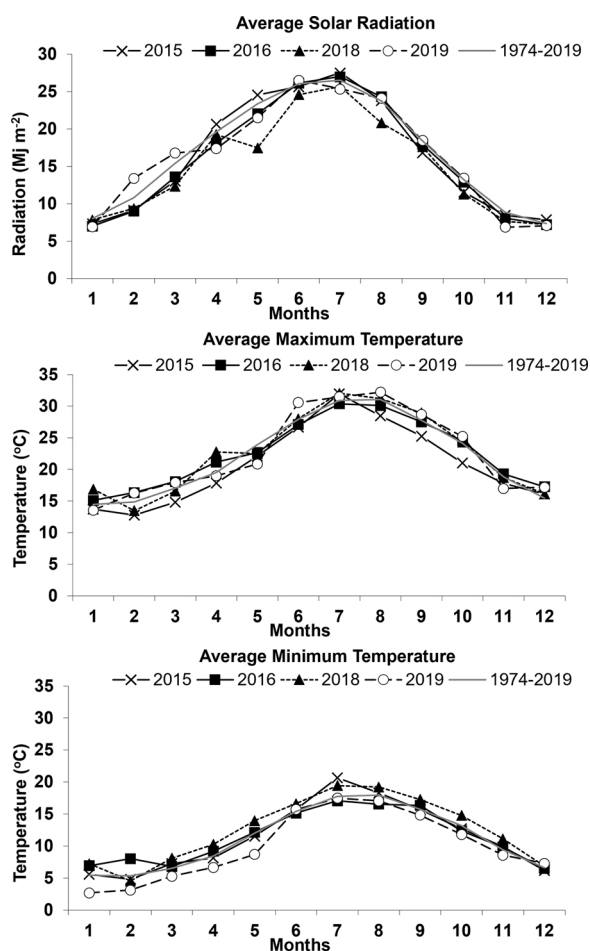


Fig. 2. Average monthly solar radiation (upper panel), maximum and minimum temperatures (middle and lower panel, respectively) recorded during the experimental years 2015, 2016, 2018, and 2019. The mean values for the three parameters, estimated from 1974 to 2019 (using all the available observations recorded at Santa Lucia), are represented by the light gray lines.

3.2. Evaluating model performance

3.2.1. Phenology, leaf area index, biomass

After calibrating the phenological parameters TSUM1 and TSUM2 for each cultivar, WOFOST is able to correctly simulate maize phenology with RMSD of 3.6 and 4.3 days for anthesis and maturity dates, respectively. The largest deviations between the simulated and the observed data occur for the earliest and latest sowing dates. The statistical coefficients indicate high level of accuracy with EF values of 0.97 and 0.96 for anthesis and maturity dates (Table 3).

Comparing simulated and observed LAI along the growing seasons points to a good agreement with an EF value of 0.78, across all the different sowing dates and cultivars. The WOFOST performance during the whole growing cycle for each cultivar and all the sowing dates is summarized in Table 3. The maximum simulated LAI ranges between 3.1 and 8.0, while the observed LAI varies between 4.8 and 10 (not shown).

WOFOST is able to correctly simulate the biomass during the growing cycle and at harvest; the RMSD for the final biomass is 4.4 t ha⁻¹. Along the growing season, the model is also able to reproduce the biomass variability associated with the different sowing dates and cultivars with RMSD of 3.3 t ha⁻¹ (Table 3).

3.2.2. Grain yield

WOFOST simulated yields range between 13.1 and 19.2 t ha⁻¹, while the observed values vary between 8.3 and 20.6 t ha⁻¹. Despite a good RMSD of 3.7 t ha⁻¹, calculated over all the cultivars and sowing dates (Table 4), the variability associated with the different sowing dates is poorly simulated as shown by the EF. The highest difference between the simulated and the observed yields characterizes the latest sowing date (7.8 t ha⁻¹).

The Otegui-Gambín simulated yield ranges between 9.4 and 15.5 t ha⁻¹. The RMSD is slightly better than the one of WOFOST (3.5 t ha⁻¹), and the yield estimation is more accurate as indicated by the positive EF and larger r^2 , showing higher responsiveness of the model to changes in sowing date and/or cultivar. The highest difference between the simulated and the observed yields is identified for the earliest sowing date (5.5 t ha⁻¹). The yield variability across the three sowing dates in 2015 and 2016, calculated using the variation coefficient *per year* and cultivar, is on average higher in Otegui-Gambín than in WOFOST (Fig. 3). As for the yield components, calculated with the Otegui-Gambín equations, the simulated number of kernels per unit area varies from 3441 to 5095, with the observed data being between 3613 and 5517. The simulated kernel weight ranges between 262 and 323 mg kernel⁻¹, while the measured values range from 219 to 341 mg kernel⁻¹.

By considering the grain filling duration together with the potential kernel growth rate and the available assimilates (during grain filling and imposing that maximum kernel weight cannot exceed the weight set

Table 3

Performance of WOFOST in terms of simulated anthesis date, maturity date, LAI, and above-ground biomass during the growing season for all the sowing dates and for all the seven cultivars (tested in the field experiments during 2015, 2016, 2018, 2019 at Santa Lucia, Sardinia, Italy). Stars represent the significance of the regression (***) $P \leq 0.001$.

	Anthesis date (DOY)	Maturity date (DOY)	LAI	Biomass (t ha ⁻¹)
RMSD	3.6	4.3	1.1	3.3
EF (1:1)	0.97	0.96	0.78	0.90
r^2	0.98***	0.97***	0.78***	0.90***
MBE	0.5	0.4	-0.25	-0.31
Slope	0.85	1.06	0.80	0.86
Intercept	30.60	-16.41	0.95	3.21
Mean observed	206	264	4.43	23.1
Mean predicted	207	264	4.59	23.2
n	31	31	960	96

Table 4

Yield performance of WOFOST and Otegui-Gambín with respect to the three sowing dates and the seven cultivars (tested in the field experiments during 2015, 2016, 2018, 2019 at Santa Lucia, Sardinia, Italy). Stars represent the significance of the estimated linear regression (* $P \leq 0.05$; *** $P \leq 0.001$).

Yield (t ha ⁻¹)	WOFOST (t ha ⁻¹)	Otegui-Gambín (t ha ⁻¹)
RMSD	3.7	3.5
EF (1:1)	0.02	0.2
MBE	1.6	-1.8
r ²	0.22*	0.46***
Slope	0.16	0.29
Intercept	14.32	8.98
Mean observed	15.1	15.1
Mean predicted	16.7	13.3
n	31	31

around flowering), the estimated kernel weight at maturity (effective kernel weight) coincides with the one calculated around flowering.

3.2.3. Yield response to sowing date and cultivar under current climate

The flowering time simulated by WOFOST varies across the tested sowing dates and cultivars along the 45 years of historical meteorological data, ranging between the 9th of June and the 5th of September

(cultivar 300 and cultivar 800, respectively).

By delaying the sowing date from April to June, comparable decreasing yield reductions are simulated by the two modelling approaches. Potential simulated yields vary on average from 10.9 to 23.0 t ha⁻¹ and from 7.6 t ha⁻¹ to 18.2 t ha⁻¹ in WOFOST and Otegui-Gambín, respectively. The lowest and the highest values are obtained for the latest and earliest sowing dates in both approaches. Grain yield differences between the first and the last sowing date diminish with the use of longer-to-reach maturity cultivar in both approaches (not shown).

Yield variability across the six sowing dates, calculated using the variation coefficient *per* year and cultivar, is higher in Otegui-Gambín than in WOFOST (Fig. 3). However, in both approaches cultivar 300 shows the highest yield variability.

For each sowing date (starting from 1 on the 15th of April and continuing till 6, 30th of June, with a 15-day interval), and for both approaches, the differences among cultivars are lower than the differences among the sowing dates with fixed cultivar (Figs. 3 and 4). Maize yield variability associated with the six cultivars and for each sowing date is higher in Otegui-Gambín, especially for the latest cultivar (Fig. 4). The lowest and the highest WOFOST-simulated values are reached with cultivars 400 and 300, respectively; while, these records are reached with cultivars 300 and 700 in Otegui-Gambín. Overall, considering the entire 45-year period, the lowest and the highest yields

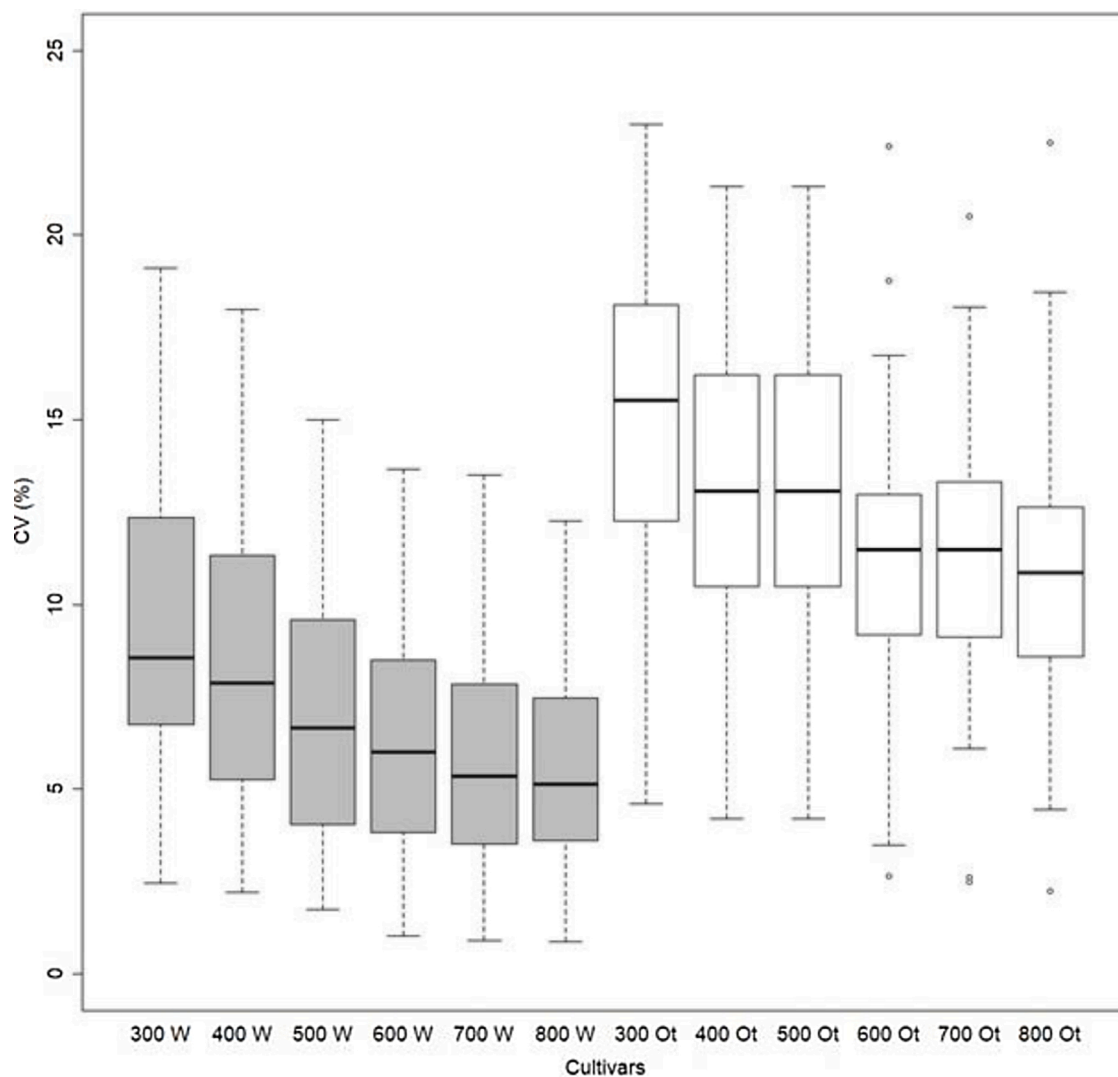


Fig. 3. Box-plots of the variation coefficients estimated for the simulated (1974-2019) maize yields using all the different sowing dates for each cultivar type (300, 400, 500, 600, 700, 800). White and grey boxplots correspond to WOFOST (W) and Otegui-Gambín (Ot), respectively.

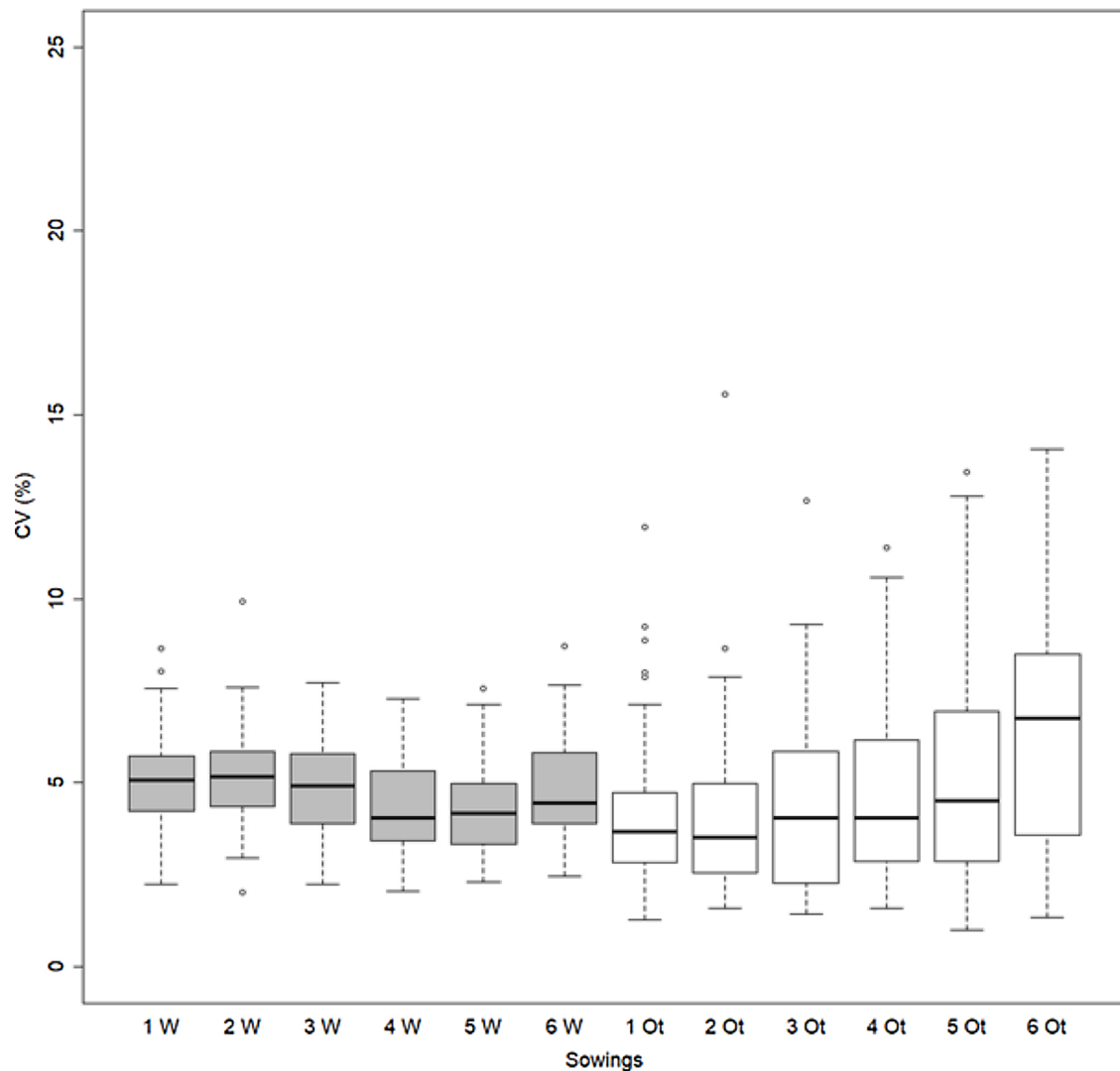


Fig. 4. Box-plots of the variation coefficients estimated for the simulated (1974-2019) maize yields using all the cultivars for each sowing date (from 1 to 6). White and grey boxplots correspond to WOFOST (W) and Otegui-Gambín (Ot), respectively.

are simulated on average: for cultivar 400 with the latest sowing and for cultivar 300 with the earliest sowing by WOFOST; for cultivar 300 with the latest sowing and for cultivar 700 with the earliest sowing by Otegui-Gambín.

The WOFOST-simulated yield variability, associated with the six sowing dates, is driven by the length of the period from flowering to maturity (Table 5); while, in Otegui-Gambín it is mostly driven by the amount of IPAR per m^2 around flowering (Table 6). The IPAR per m^2 variability among sowing dates is also correlated with the variability of biomass at flowering. However, the Otegui-Gambín simulated yield variability (as a response to varying sowing dates) is only partially explained by the maximum LAI. Variability of biomass at flowering and maximum LAI show lower effects on WOFOST-simulated yield

variability (induced by varying the sowing dates).

Final kernel weight at maturity coincides with the weight set around flowering. Assimilates from remobilization contribute on average 9% to the final kernel weight, with the highest value (24%) achieved by the latest cultivar. The traslocated part of kernel weight has minor importance in comparison with the available traslocates.

By analyzing the yield cumulative distribution function, it emerges that the highest probability of the highest yield is achieved by WOFOST with cultivar 300 (not shown). The cumulative distribution functions estimated for the Otegui-Gambín simulations show less pronounced differences between cultivars; on the contrary, differences between the sowing dates are higher.

Table 5

Spearman correlation and associated significance estimated for the variation coefficient (CV) of the WOFOST-simulated yields and the CV of: the number of days from flowering to maturity; the IPAR per m^2 around flowering; the biomass at flowering; the maximum LAI. CVs are all calculated among the six sowing dates.

Variation coefficient (%) of yields simulated by WOFOST	CV 300	CV 400	CV 500	CV 600	CV 700	CV 800
Days from flowering to maturity	−0.74***	−0.68***	−0.75***	−0.67***	−0.58***	−0.52**
IPAR m^{-2} around flowering	n.s.	n.s.	n.s.	n.s.	n.s.	n.s.
Biomass at flowering	n.s.	n.s.	n.s.	n.s.	n.s.	−0.33*
Maximum LAI	n.s.	n.s.	n.s.	n.s.	n.s.	−0.31*

Table 6

Spearman correlation and associated significance estimated for the variation coefficient (CV) of the Otegui-Gambín simulated yields and the CV of: the number of days from flowering to maturity; the IPAR per m² around flowering; the biomass at flowering; the maximum LAI. CVs are all calculated among the six sowing dates.

Variation coefficient (%) of yields simulated by Otegui-Gambín						
CV (%)	CV 300	CV 400	CV 500	CV 600	CV 700	CV 800
Days from flowering to maturity	n.s.	n.s.	n.s.	n.s.	n.s.	n.s.
IPAR m ⁻² around flowering	0.98***	0.98***	0.98***	0.95***	0.96***	0.97***
Biomass at flowering	0.75***	0.60***	0.52**	0.44**	0.37*	0.32*
Maximum LAI	0.55***	0.40**	0.31*	n.s.	n.s.	n.s.

3.3. Yield response under future climate conditions

Figs. 5 and 6 show the simulated maize yield variability induced by changes in the sowing date for all the tested cultivars during the baseline and in the two future time periods (2021–2040 and 2041–2060 under the RCP8.5 scenario). Under the projected climate conditions, increased maize yield variability is simulated by both modelling approaches. However, higher coefficient of variability (as a response to the six different sowing dates) is simulated by Otegui-Gambín. Cultivar 300 exhibits the highest projected yield variability, independently from the considered RCM/GCM and yield modelling approach; while, cultivar 800 (similarly 600 and 700) shows the lowest variability.

Future maize yield is projected to decrease compared to the baseline period, independently from: the climate model (not shown), the yield modelling approach, the cultivar and the sowing date (Fig. 7). Results show that, with no adaption maize yield will decrease across all sowing dates and cultivars by on average 9 % and 17 % (2021–2040 and 2041–2060 vs the baseline, respectively) according to WOFOST, and by

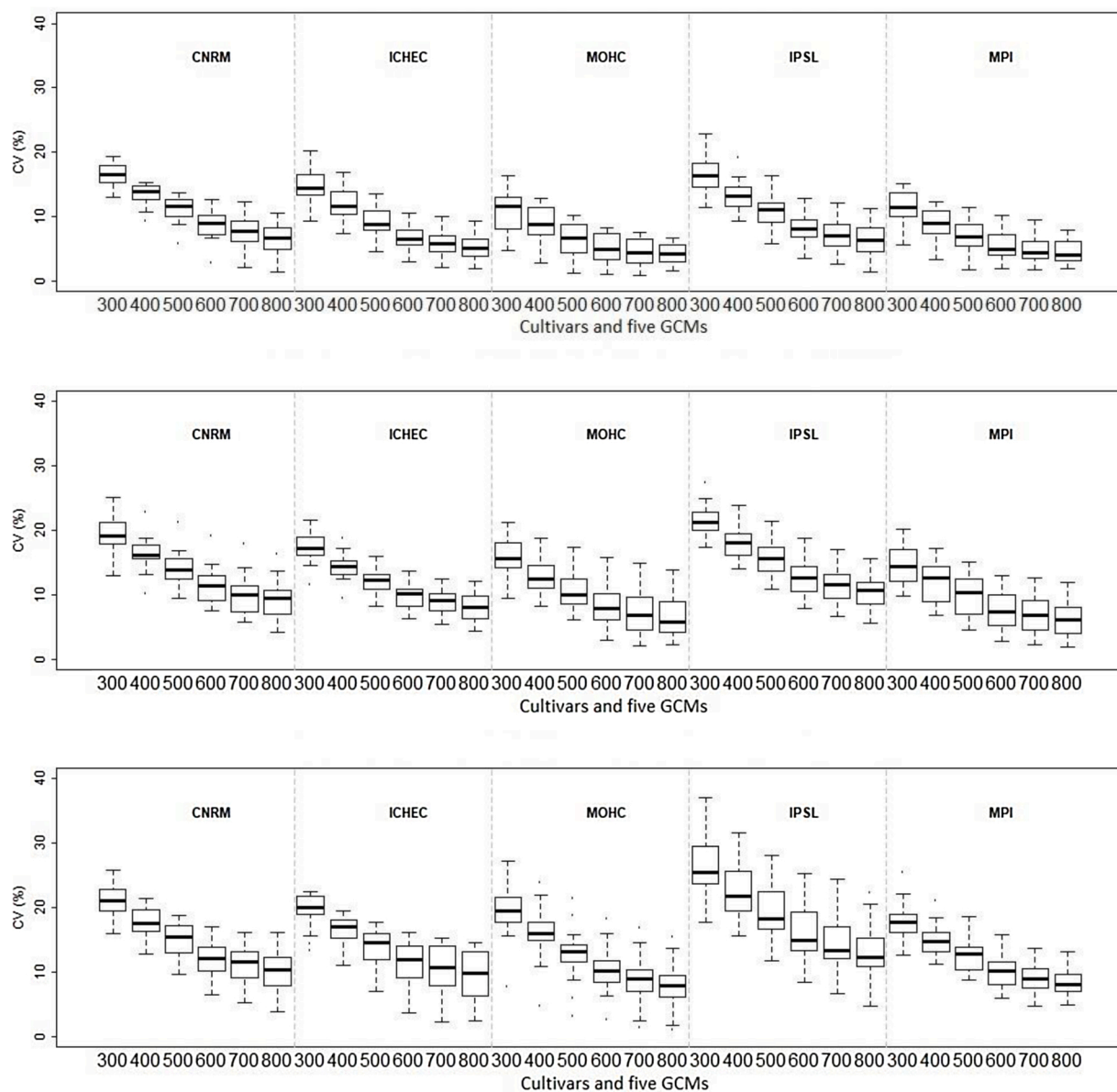


Fig. 5. Box-plots of the variation coefficients estimated for the WOFOST-simulated maize yields using all the six sowing dates for each cultivar type (300, 400, 500, 600, 700, 800) during the following periods: 1986-2005 (historical), 2021-2040 (RCP8.5), 2041-2060 (RCP8.5). The RCM-GCM combinations are identified with the short name of the driving GCM.

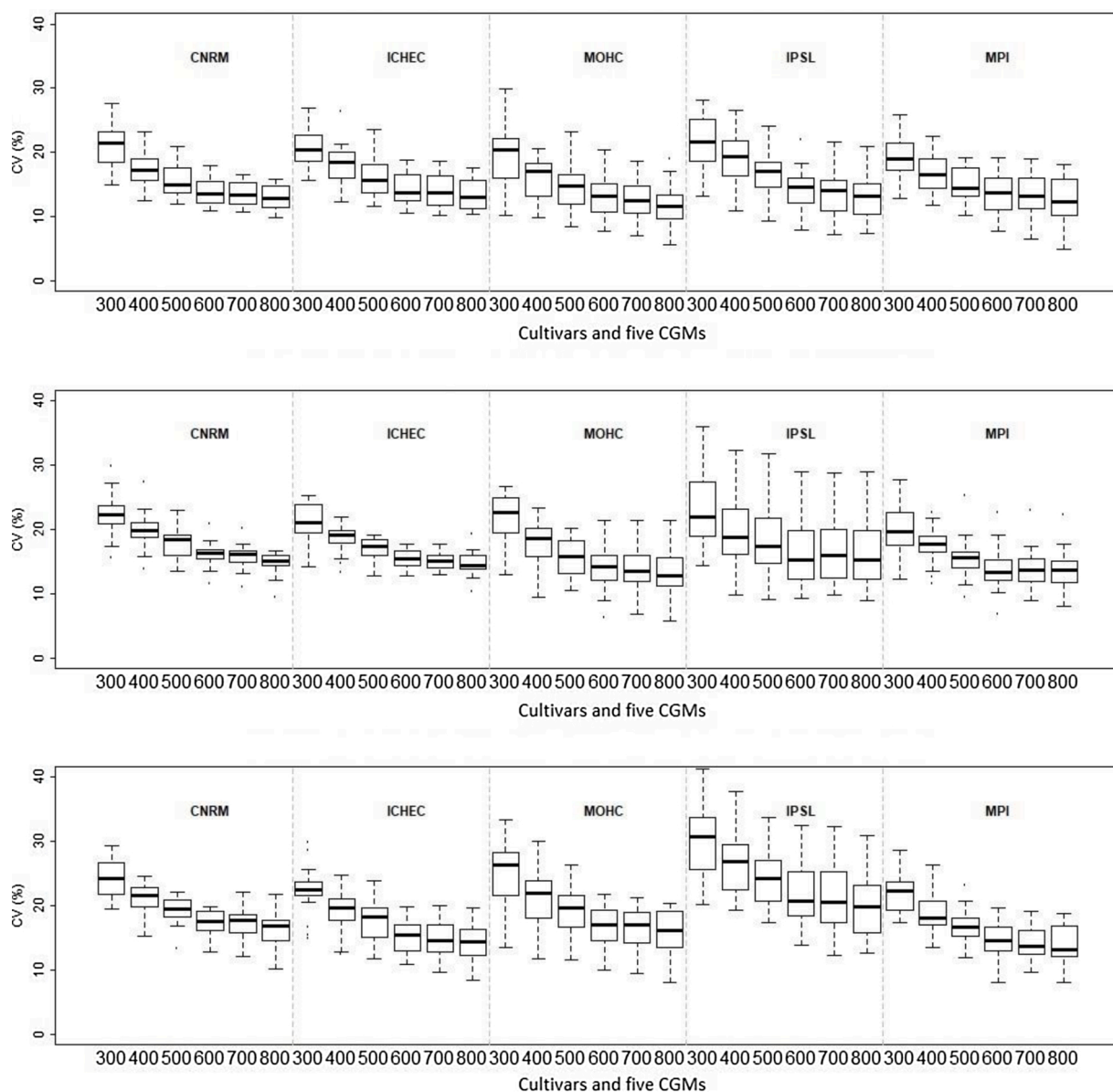


Fig. 6. Box-plots of the variation coefficients estimated for the Otegui-Gambín simulated maize yields using all six sowing dates for each cultivar type (300, 400, 500, 600, 700, 800) during the following periods: 1986-2005 (historical), 2021-2040 (RCP8.5), 2041-2060 (RCP8.5). The RCM-GCM combinations are identified with the short name of the driving GCM.

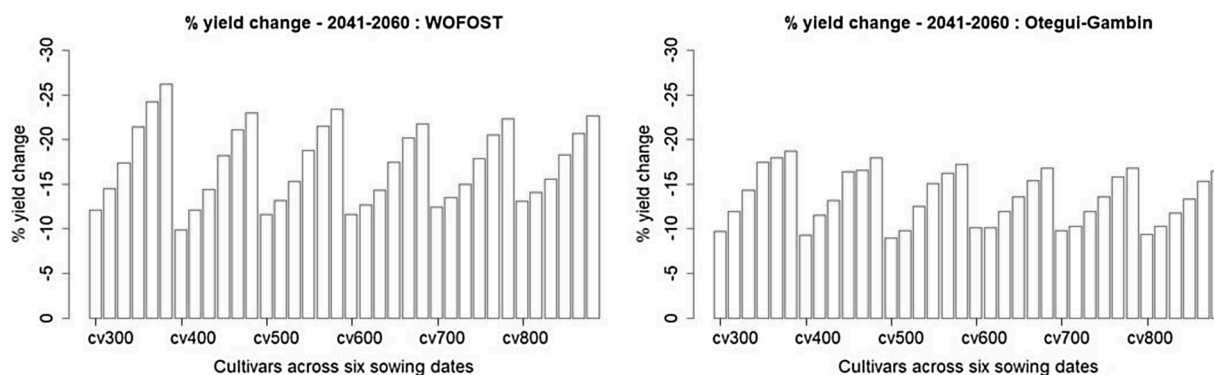


Fig. 7. Impact of the different sowing dates and cultivar on crop yield response to climate change. Bar-plots show, for both WOFOST (left panel) and Otegui-Gambín (right panel), the RCM/GCM ensemble mean yield change estimated for 2041-2060 (expressed in % with respect to the 1986-2005 baseline period).

7 % and 14 % (2021–2040 and 2041–2060 vs the baseline, respectively) according to Otegui-Gambín.

Simulated yield responses differ among the five RCM/GCM combinations (as also reported by, e.g., Rummukainen, 2016). Indeed, the projected yield reductions in 2041–2060 vary on average from 5 % to 37 % by using WOFOST and between 2 % and 30 % by using Otegui-Gambín. The highest projected mean yield reduction is simulated by both approaches with cultivar 300 and using the latest sowing date. The lowest projected mean yield reduction is projected with cultivars 400 and 500 by using the earliest sowing date in, respectively, WOFOST and Otegui-Gambín.

4. Discussion

The main findings of this study reveal that WOFOST is able to simulate phenology, growth, and average maize yield. The simulated maize yields across the long-term historical period 1974–2019, covered by local meteorological records, are in the range of simulated maize potential yields in Europe (Schils et al., 2018). However, the error in the WOFOST-simulated grain yield increases when different sowing dates and cultivars are considered.

Despite the importance of crop model responses to changes in sowing date and cultivar, models' processes representations have been rarely explored (Hammer and Broad, 2003; Messina et al., 2009; Bonelli et al., 2016). Our results show that Otegui-Gambín, an alternative yield modelling approach (based on yield components, plant growth rate, and intercepted light averaged over a critical period around flowering) outperforms WOFOST in reproducing the observed variability associated with the tested sowing dates. The significant linear relationship (established between the number of kernels *per* plant and the IPAR *per* plant during a well-defined critical period in field experiments conducted in France and in Argentina; Otegui and Bonhomme, 1998) resulted valid for a wide range of growing conditions, including different sowing dates and latitudes. Independently from the environment and the genotype, our results confirm that the linear regression found by Otegui and Bonhomme (1998) is valid and achieves good yield accuracy also in a Mediterranean environment. Accordingly, our results further validate the ones of Gambín et al. (2006), confirming that a simple and mechanistic source-sink ratio estimation around flowering determines the final maize kernel weight.

This supports the understanding that fully irrigated maize yields in the Mediterranean environment are mainly limited by source availability during early flowering (determining maize potential sink capacity) rather than being limited by the biomass *per* kernel produced during the effective grain filling period and by its duration (Gambín et al., 2006).

Despite a varying duration of the grain filling period across the tested sowing dates and cultivars, this study shows that simple relationship established around flowering leads to an accurate estimate of the effect of sowing date on maize potential grain yield. Our analysis, indeed, reveals that crop conditions around flowering time are able to explain maize yield variation in response to different sowing dates and cultivars. This can be understood by considering that in absence of environmental constraints (such as water shortage, frost, and heat stress) yield is solely determined by radiation and temperature during the growth critical period (Andrade et al., 2010). For all the sowing dates, kernel growth during the grain filling was limited by the sink strength set around flowering time, independently of the temperature variation during the grain filling. When grain filling was also considered, and thus photosynthetic source capacity became a limiting factor, grain growth was supported by remobilization of carbohydrates. This is in agreement with the results of Bonelli et al. (2016) who found that grain growth with late sowing dates (when lower temperatures reduce assimilation) was limited by photosynthetic source capacity although supported by remobilization of carbohydrates. Similarly, other studies identified maize as the crop having the largest capacity to buffer changes in

assimilates availability during grain filling (Andrade and Ferreiro, 1996). According to Andrade and Ferreiro (1996) maize yields are partially dependent on crop condition during grain filling. Shorter grain filling, induced by higher temperatures, may not affect yield when compensated by higher incident daily radiation (Muchow, 1990).

In agreement with previous results (e.g. Borrás et al., 2004), our simulated yield resulted mainly sink limited in all the explored growing conditions. The kernel weight set at flowering limits the kernel weight achievable with the available assimilates during grain filling (in agreement with Otegui et al., 1995). If the assimilates availability from actual photosynthesis during grain filling plus reserve remobilization exceed the demand from the growing grains, yield improvement may come from sink strength increase around flowering (Borrás et al., 2004). Therefore, even if grain filling occurs under environmental conditions less favorable than those experienced during seed set (with assimilates from photosynthesis below the point saturating maximum kernel weight), remobilization of assimilates (temporarily stored in stems and leaves) for grain production is an important factor determining kernel weight. Our results suggest that a small source variation during the maize yield critical period has greater effect on potential yield than changes in source capacity during grain filling (Andrade and Ferreiro, 1996).

In terms of response to varying sowing dates, WOFOST and Otegui-Gambín show similar behavior, with the earliest cultivar showing the highest yield variability. This response is projected to be amplified by climate change, with the earliest cultivar still showing the highest variability across different sowing dates (in agreement with Torriani et al., 2007; Zhu et al., 2018). However, the highest variability is not associated with higher mean yield, which is achieved by the earliest sowing date independently from the cultivar.

Our analysis shows that, in absence of other yield-reducing factors (such as nutrients, water, and killing frost), the effect of sowing date is larger than the effect of the cultivar on yield, and the highest yield can be achieved with early sowings (in agreement with Long et al., 2017; Baum et al., 2019). This implies that the cultivar choice has minor effect on yield, in agreement with other experimental data and studies (e.g. Baum et al., 2019) that attributed most of the yield variability to sowing dates (as long as cultivars reach maturity before harvesting).

Under future climate conditions, maize productivity is projected to decrease, independently from the climate model and the crop modelling approach. We estimated average yield reductions up to 17 %, similarly to Tubiello et al. (2000) and Xu et al. (2016).

Recommendations to cope with the impacts of global climate change include early sowing (Giannakopoulos et al., 2009). In our results, indeed, the early sowing date shows the lowest yield reduction. At the same time, according to Otegui-Gambín, cultivars with longer growing cycle show a yield-advantage. The use of longer growing cycle cultivars has been reported as a worthy adaptation strategy in warmer climate conditions, where higher temperatures increase crop development rate (Giannakopoulos et al., 2009; Liu et al., 2013; Ma et al., 2017; Zhu et al., 2018). However, Zhu et al. (2018) found that the negative impacts of climatic warming can be only partially offset with such an adaptation strategy.

5. Conclusions

Many studies explored the impacts of changes in sowing date and cultivar on maize yield, without questioning the method used for the evaluation. Here, we investigated the yield partitioning crop formalism to understand its adequateness in representing crop yield variability in response to changing sowing dates and cultivars. Our findings show that the partitioning approach achieves less accurate yield estimates across different sowing dates; whereas, an approach based on the anthesis conditions and yield components performs better.

Concerning the coming decades (up to 2060) and the responses under future climate conditions, both modelling approaches agree on

the negative yield effects of climate change being only partially alleviated by changing cultivar and sowing date. Other changes in traits and/or management practices will be needed.

Our study represents an initial assessment to identifying approaches that may better explain yield variability in response to changes in environmental conditions and agro-management practices. The results, here discussed, would need further evaluations before being considered applicable outside the analyzed conditions. To this aim, the new modelling approach has been also integrated into the MARS Crop Yield Forecasting System to monitor maize yield in potential conditions across different environments. Additional evaluations should be also performed by replacing WOFOST with other crop growth models, to sample the full range of uncertainties with respect to the yield responses here investigated.

Declaration of Competing Interest

The authors report no declarations of interest.

Acknowledgements

We thank Paola Fenu, Roberto Leri, and Paolo Manca for their technical assistance. We also thank Matteo Serusi for the additional year of field data used in the calibration of WOFOST.

The research has been conducted at the Joint Research Centre. The University of Sassari contributed in part to the research. "Università di Sassari" and "Fondo di Ateneo per la Ricerca 2019" for BOTH Francesco Giunta and Rosella Motzo.

Appendix A. Supplementary data

Supplementary material related to this article can be found, in the online version, at doi:<https://doi.org/10.1016/j.fcr.2021.108226>.

References

- Allen, R.G., Pereira, L.S., Raes, D., Smith, M., 1998. *Crop Evapotranspiration: Guidelines for Computing Crop Water Requirements*. FAO Irrigation and Drainage Paper 56. FAO, Rome, 300 pp.
- Anapalli Saseendran, S., Ma, L., Nielsen, D.C., Vigil, M.F., Ahuja, L.R., 2005. Simulating planting date effects on corn production using RZWQM and CERES-maize models. *Agron. J.* 97, 58–71.
- Andrade, F.H., Ferreiro, M.A., 1996. Reproductive growth of maize, sunflower and soybean at different source levels during grain filling. *Field Crops Res.* 48, 155–165.
- Andrade, F.H., Abbate, P.E., Otegui, M.E., Cirilo, A.G., Cerrudo, A.A., 2010. Ecophysiological bases for crop management. *Am.J.P.S.B.* 4, 23–34.
- Baum, M.E., Archontoulis, S.V., Licht, M.A., 2019. Planting date, hybrid maturity, and weather effects on maize yield and crop stage. *Agron. J.* 111, 1–11.
- Bonelli, L.E., Monzon, J.P., Cerrudo, A., Rizzalli, R.H., Andrade, F.H., 2016. Maize grain yield components and source-sink relationship as affected by the delay in sowing date. *Field Crops Res.* 198, 215–225.
- Boogaard, H.L., Van Diepen, C.A., Rotter, R.P., Cabrera, J.M.C.A., Van Laar, H.H., 1998. *User's Guide for the WOFOST 7.1 Crop Growth Simulation Model and WOFOST Control Center 1.5*. DLO Winand Staring Centre, Wageningen (Netherlands).
- Boons-Prins, E.R., deKoning, G.H.J., van Diepen, C.A., de Vries, P., 1993. *Crop Specific Simulation Parameters for Yield Forecasting Across the European Community*. Simulation Reports CABO-IT.No.32. CABO-DLO Wageningen Agricultural University, Wageningen.
- Boote, K.J., et al., 1999. Concepts for calibrating crop growth models. In: Tsujii, G.Y. (Ed.), *DSSAT Version 3*. Vol. 4-6. International Benchmark Sites Network for Agrotechnology Transfer. Univ. of Hawaii, Honolulu, HI, pp. 179–200.
- Borrás, L., Slafer, G.A., Otegui, M.E., 2004. Seed dry weight response to source-sink manipulations in wheat, maize and soybean: a quantitative reappraisal. *Field Crops Res.* 86, 131–146.
- Caviglia, O.P., Melchiori, R.J.M., Sadras, V.O., 2014. Nitrogen utilization efficiency in maize as affected by hybrid and N rate in late-sown crops. *Field Crops Res.* 168, 27–37.
- Ceglar, A., Crepinsek, Z., Kajfez-Bogataj, L., Pogacar, T., 2011. The simulation of phenological development in dynamic crop model: the Bayesian comparison of different methods. *Agric. For. Meteorol.* 151, 101–115.
- Cirilo, A.G., Andrade, F.H., 1994. Sowing date and maize productivity: I. Crop growth and dry matter partitioning. *Crop Sci.* 34, 1039–1043.
- Ciscar, J.C., Ibarreta, D., Soria, A., Dosio, A., Toreti, A., Ceglar, A., Fumagalli, D., Dentener, F., Leclerc, R., Zucchini, A., Panarello, L., Niemeier, S., Pérez-Domínguez, I., Fellmann, T., Kitous, A., Després, J., Christodoulou, A., Demirel, H., Alfieri, L., Dottori, F., Voutsoukas, M.I., Mentaschi, L., Voukouvalas, E., Cammalleri, C., Barbosa, P., Micale, F., Vogt, J.V., Barredo, J.I., Caudullo, G., Mauri, A., de Rigo, D., Libertà, G., Houston Durrant, T., Artés Vivancos, T., San-Miguel-Ayanz, J., Gosling, S.N., Zaherpour, J., De Roo, A., Bisselink, B., Bernhard, J., Bianchi, L., Rozsai, M., Szewczyk, W., Mongelli, I.L., Feyen, L., 2018. *Climate Impacts in Europe: Final Report of the JRC PESETA III Project*, EUR 29427 EN. Publications Office of the European Union, Luxembourg, p. 2018. ISBN 978-92-79-97218-8.
- De Koning, G.H.J., Van Diepen, C.A., 1992. *Crop Production Potential of Rural Areas Within the European Communities. IV. Potential, Water-limited and Actual Crop Production*. Working Document W68, Netherlands Scientific Council for Government Policy, the Hague, The Netherlands.
- Dosio, A., 2016. Projections of climate change indices of temperature and precipitation from an ensemble of bias-adjusted high-resolution EURO-CORDEX regional climate models. *J. Geophys. Res. Atmos.* 121, 5488–5511.
- Echarte, L., Andrade, F.H., 2003. Harvest index stability of Argentinean maize hybrids released between 1965 and 1993. *Field Crops Res.* 82, 1–12.
- Echarte, L., Andrade, F.H., Sadras, V.O., Abbate, P., 2006. Kernel weight and its response to source manipulations during grain filling in Argentinean maize hybrids released in different decades. *Field Crop Res.* 96, 307–312.
- Gambín, B.L., Borrás, L., Otegui, M.E., 2006. Source-sink relations and kernel weight differences in maize temperate hybrids. *Field Crops Res.* 95, 316–326.
- Genovesi, G., Bettio, M. (Eds.), 2004. *Methodology of the MARS Crop Yield Forecasting System*. Statistical Data Collection, Processing and Analysis, vol. 4. European Communities, Luxembourg. ISBN 92-894-8183-8188.
- Giannakopoulos, C., Le Sager, P., Bindi, M., Moriondo, M., Kostopoulou, E., Goodess, C. M., 2009. Climatic changes and associated impacts in the Mediterranean resulting from a 2 °C global warming. *Global Planet. Change* 68, 209–224.
- Grassini, P., Thorburn, J., Burr, C., Cassman, K.G., 2011. High-yield irrigated maize in the Western U.S. corn belt: I. On-farm yield, yield potential, and impact of agronomic practices. *Field Crops Res.* 120, 142–150.
- Hammer, G.L., Broad, J.J., 2003. Genotype and environment effects on dynamics of harvest index during grain filling in sorghum. *Agron. J.* 95, 199–206.
- Hristov, J., Toreti, A., Perez Dominguez, I., Dentener, F., Fellmann, T., Elleby, C., Ceglar, A., Fumagalli, D., Niemeier, S., Cerrani, I., Panarello, L., Bratu, M., 2020. *Analysis of Climate Change Impacts on EU Agriculture by 2050*, EUR 30078 EN. Publications Office of the European Union, Luxembourg. <https://doi.org/10.2760/121115,JRC119632>. ISBN 978-92-76-10617-3.
- Jacob, D., Petersen, J., Eggert, B., Alias, A., Christensen, O.B., Bouwer, L.M., Braun, A., Colette, A., Déqué, M., Georgievski, G., Georgopoulou, E., Gobiet, A., Menut, L., Nikulin, G., Haensler, A., Hempelmann, N., Jones, C., Keuler, K., Kovats, S., Kröner, N., Kotlarski, S., Kriegsmann, A., Martin, E., van Meijgaard, E., Moseley, C., Pfeifer, S., Preuschmann, S., Radermacher, C., Radtke, K., Reich, D., Rounsevell, M., Samuelsson, P., Somot, S., Soussana, J.-F., Teichmann, C., Valentini, R., Vautard, R., Weber, B., Yiou, P., 2014. EURO-CORDEX: new high-resolution climate change projections for European impact research. *Reg. Environ. Change* 14, 563–578.
- Jugenheimer, R.W., 1958. Hybrids maize breeding and seed production. *FAO Agric. Dev. Pop.* 62, 99–103.
- Lazar, C., Genovesi, G. (Eds.), 2004. *Methodology of the MARS Crop Yield Forecasting System*. Agrometeorological Data Collection, Processing and Analysis, vol. 2. European Communities, Luxembourg. ISBN 92-894-8181-1.
- Liu, Z., Hubbard, K.G., Lin, X., Yang, X., 2013. Negative effects of climate warming on maize yield are reversed by the changing of sowing date and cultivar selection in Northeast China. *Glob. Change Biol.* 19, 3481–3492.
- Long, N.V., Assaifa, Y., Schwalbert, R., Ciampitti, I.A., 2017. Maize yield and planting date relationship: a synthesis-analysis for US high-yielding contest-winner and field research data. *Front. Plant Sci.* 8 (2106), 1–9.
- Ma, L., Ahuja, L.R., Islam, A., Trout, T.J., Saseendran, S.A., Malone, R.W., 2017. Modeling yield and biomass responses of maize cultivars to climate change under full and deficit irrigation. *Agric. Water Manage.* 180, 88–98.
- Messina, C., Hammer, G., Dong, Z., Poddich, D., Cooper, M., 2009. Modelling crop improvement in a GxExM framework via gene-trait-phenotype relationships. In: Sadras, V., Calderini, D. (Eds.), *Crop Physiology: Applications for Genetic Improvement and Agronomy*. Elsevier, The Netherlands, pp. 235–265.
- Micale, F., Genovesi, G., 2004. *Methodology of the MARS Crop Yield Forecasting System*. Meteorological Data Collection, Processing and Analysis, vol. 1. European Communities (EUR 21291 EN), Luxembourg.
- Monteith, J.L., 1965. Radiation and crops. *Exp. Agric.* 1, 241–251.
- Muchow, R.C., 1990. Effect of high temperature on grain-growth in field-grown maize. *Field Crops Res.* 23, 145–158.
- Olesen, J.E., Bindi, M., 2002. Consequences of climate change for European agricultural productivity, land use and policy. *Eur. J. Agron.* 16, 239–262.
- Otegui, M.E., Bonhomme, R., 1998. Grain yield components in maize I. Ear growth and kernel set. *Field Crop Res.* 56, 247–256.
- Otegui, M.E., Nicolini, M.G., Ruiz, R.A., Dodds, P.A., 1995. Sowing date effects on grain yield components of different maize genotypes. *Agron. J.* 87, 29–33.
- Otegui, M., Ruiz, R.A., Petrucci, D., 1996. Modeling hybrid and sowing date effects on potential grain yield of maize in a humid temperate region. *Field Crops Res.* 47, 167–174.
- Riahi, K., Rao, S., Krey, V., Cho, C., Chirkov, V., Fischer, G., Kindermann, G., Nakicenovic, N., Rafaj, P., 2011. RCP 8.5 - a scenario of comparatively high greenhouse gas emissions. *Clim. Change* 109, 33–57.
- Ritchie, J.T., NeSmith, D.S., 1991. Temperature and crop development. In: Hanks, J., Ritchie, J.T. (Eds.), *Modelling Plant and Soil Systems*, Agronomy Series 31. ASA-CSSA-SSSA, Madison, pp. 5–29.

- Rummukainen, M., 2016. Added value in regional climate modeling. *WIREs Clim Change* 7, 145–159.
- Srivastava, R.K., Panda, R.K., Chakraborty, A., Halder, D., 2018. Enhancing grain yield, biomass and nitrogen use efficiency of maize by varying sowing dates and nitrogen rate under rainfed and irrigated conditions. *Field Crops Res.* 221, 339–349.
- Supit, I., Van Diepen, C.A., De Wit, A.J.W., Kabat, P., Baruth, B., Ludwig, F., 2010. Recent changes in the climatic yield potential of various crops in Europe. *Agric. Syst.* 103, 683–694.
- Supit, I., Van Diepen, C.A., De Wit, A.J.W., Wolf, J., Kabat, P., Baruth, B., Ludwig, F., 2012. Assessing climate change effects on European crop yields using the Crop Growth Monitoring System and a weather generator. *Agric. Forest Meteorol.* 164, 96–111.
- Tojo Soler, C.M., Sentelhas, P.C., Hoogenboom, G., 2007. Application of the CSM-CERES-Maize model for planting date evaluation and yield forecasting for maize grown off-season in a subtropical environment. *Eur. J. Agron.* 27, 165–177.
- Torriani, D.S., Calanca, P., Schmid, S., Beniston, M., Fuhrer, J., 2007. Potential effects of changes in mean climate and climate variability on the yield of winter and spring crops in Switzerland. *Clim. Chang. Res. Lett.* 34, 59–69.
- Tsimba, R., Edmeades, G.O., Millner, J.P., Kemp, P.D., 2013a. The effect of planting date on maize grain yields and yield components. *Field Crops Res.* 150, 135–144.
- Tsimba, R., Edmeades, G.O., Millner, J.P., Kemp, P.D., 2013b. The effect of planting date on maize: phenology:thermal time durations and growth rates in a cool temperate climate. *Field Crops Res.* 150, 145–155.
- Tubiello, F.N., Donatelli, M., Rosenzweig, C., Stockle, C.O., 2000. Effects of climate change and elevated CO₂ on cropping systems: model predictions at two Italian locations. *Eur. J. Agron.* 13, 179–189.
- Van Diepen, C.A., Wolf, J., Van Keulen, H., Rappoldt, C., 1989. WOFOST: a simulation model of crop production. *Soil Use Manage.* 5, 16–24.
- Vučetić, V., 2011. Modelling of maize production in Croatia: present and future climate. *J. Agric. Sci.* 149, 145–157.
- Willmott, C.J., 1982. Some comments on the evaluation of model performance. *Bull. Am. Meteorol. Soc.* 63, 1309–1313.
- Wolf, J., 1993. Effects of climate change on wheat production potential in the European Community. *Eur. J. Agron.* 2, 281–292.
- Wolf, J., Van Diepen, C.A., 1995. Effects of climate change on grain maize yield potential in the European Community. *Clim. Change* 29, 299–331.
- Xu, H., Twine, T.E., Girvetz, E., 2016. Climate change and maize yield in Iowa. *PLoS One* 11, 1–20.
- Yang, H., Dobermann, A., Cassman, K.G., Walters, D.T., 2006. Features, applications, and limitations of the hybrid-maize simulation model. *Agron. J.* 98, 737–748.
- Zhao, J., Yang, X., Dai, S., Lv, S., Wang, J., 2015. Increased utilization of lengthening growing season and warming temperatures by adjusting sowing dates and cultivar selection for spring maize in Northeast China. *Eur. J. Agron.* 67, 12–19.
- Zhou, B., Yue, Y., Sun, X., Ding, Z., Ma, W., Zhao, M., 2017. Maize kernel weight responses to sowing date-associated variation in weather conditions. *Crop J.* 5, 43–51.
- Zhu, P., Jin, Z., Zhuang, Q., Ciaia, P., Bernacchi, C., Wang, X., Makowski, D., Lobell, D., 2018. The important but weakening maize yield benefit of grain filling prolongation in the US Midwest. *Glob. Change Biol.* 24, 4718–4730.